Vol 18 No 2, February 2009
1674-1056/2009/18(02)/0506-10

Chinese Physics B

© 2009 Chin. Phys. Soc.
and IOP Publishing Ltd

Emergence of spatiotemporal chaos arising from far-field breakup of spiral waves in the plankton ecological systems*

Liu Quan-Xing(刘权兴)[a], Sun Gui-Quan(孙桂全)[a], Jin Zhen(靳 祯)[a]†, and Li Bai-Lian(李百炼)[b]

[a] *Department of Mathematics, North University of China, Taiyuan, 030051, China*
[b] *Ecological Complexity and Modeling Laboratory, Department of Botany and Plant Sciences, University of California, Riverside, CA 92521-0124, USA*

(Received 4 April 2008; revised manuscript received 22 September 2008)

It has been reported that the minimal spatially extended phytoplankton–zooplankton system exhibits both temporal regular/chaotic behaviour, and spatiotemporal chaos in a patchy environment. As a further investigation by means of computer simulations and theoretical analysis, in this paper we observe that the spiral waves may exist and the spatiotemporal chaos emerge when the parameters are within the mixed Turing–Hopf bifurcation region, which arises from the far-field breakup of the spiral waves over a large range of diffusion coefficients of phytoplankton and zooplankton. Moreover, the spatiotemporal chaos arising from the far-field breakup of spiral waves does not gradually invade the whole space of that region. Our results are confirmed by nonlinear bifurcation of wave trains. We also discuss ecological implications of these spatially structured patterns.

Keywords: reaction–diffusion systems, travelling wave, bifurcation
PACC: 0565, 0547

1. Introduction

There is a growing interest in the spatial pattern dynamics of ecological systems.[1−13] However, many mechanisms of the spatiotemporal variation of natural plankton populations are not known yet. Pronounced physical patterns like thermoclines, upwelling, fronts and eddies often set the frame for the biological process. Measurements of the underwater light field are made with state-of-the-art instruments and used to calculate concentrations of phytoplankton biomass (like chlorophyll) as well as other forms of organic matter. Very high diffusion of the marine environment would prevent the formation of any stable patched spatial distribution with much longer lifetime than the typical time of biodynamics. Meanwhile, in addition to very changeable transient spatial patterns, there also exist other spatial patterns in marine environment, much more stable spatial structure associated with ocean fronts, spatiotemporal chaos,[10,11,14] cyclonic rings, and the so-called meddies.[15] In fact, it is significant to create the biological basis for understanding spatial patterns of plankton.[16] For instance, the impact of space on the persistence of enriched ecological systems was proved in laboratory experiments.[17] Recently, it has been shown that the existence of a spatial structure makes a predator-prey system less prone to extinction both in laboratory experiments[18] and theoretical prediction.[14,19−21] This is explained by the fact that the temporal variations of the density of different sub-populations can become asynchronous and the events of local extinction can be compensated due to re-colonization from other sites in the space.[22] For a long period of time, all the spiral waves have been widely observed in diverse physical, chemical, and biological systems.[23−26] However, a quite limited number of publications[11,12,27−29] relate the spiral wave pattern and its breakup to the ecological systems.

The investigation of transition from regular patterns to spatiotemporally chaotic dynamics in spatially extended systems remains a challenge in non-

*Project supported by the National Natural Science Foundation of China (Grant No 60771026), the Program for New Century Excellent Talents in University (Grant No NCET050271), the Natural Science Foundation of Shan'xi Province, China (Grant No 2006011009), US National Science Foundation Biocomplexity Program (DEB0421530), and LTER Program (Grant No DEB0620482).

†Corresponding author. E-mail: jinzhn@263.net

linear science.[14,23,30,31] In a nonlinear ecological system, the two most commonly seen patterns are spiral waves and turbulence (spatiotemporal chaos) at the level of the community models.[32] It has been recently shown that spontaneous spatiotemporal pattern formation is an intrinsic property of an ecological system[11,14,33–36] and the spatiotemporal structures play an important role in ecology. For example, spatially induced speciation prevents the extinction of the predator-prey models.[11,12,37] So far, plankton patchiness has been observed in a wide range of spatiotemporal scales.[38,39] There exist various, often heuristic explanations for the spatial patterns phenomenon in these systems. It should be noted that, although conclusive evidence of ecological chaos is still to be found, there is a growing number of indications of chaos in real ecosystems.[14,40–44] In particular, Becks *et al* [44] showed that the dynamic behaviour of such a two-prey, one-predator system includes chaotic behaviour, as well as stable limit cycles and coexistence at equilibrium, in which they offered a new possibility for the experimental study of deterministic chaos in real biological systems by defining a microbial food web.

Recently developed models show that spatial self-structuring in multi-species systems can meet both criteria and provide a rich substrate for community-level section and a major transition in evolution. In present paper, the scenario in the spatially extended plankton ecological system is observed by means of numerical simulation. The system has been demonstrated to exhibit regular or chaotic patterns, depending on the initial conditions and the parameter values.[10,29] We find that the far-field breakup of the spiral waves leads to complex spatiotemporal chaos (or a turbulent-like state) in the spatially extended plankton model. Our results show that regular spiral wave pattern shifts into spatiotemporal chaos pattern by modulating the diffusion coefficients of the species.

2. Model

In this paper we study the spatially extended nutrient–phytoplankton–zooplankton–fish reaction–diffusion system. Following Scheffer's minimal approach,[45] which was originally formulated as a system of ordinary differential equations (ODEs), and the previous analysis,[10,11,29,33,46,47] we study a two-variable phytoplankton and zooplankton model at the level of the community to describe pattern formation with diffusion. The original spatially extended model is written as

$$\frac{\partial P}{\partial t} = RP\left(1-\frac{P}{K}\right) - \frac{A_1 C_1 P}{C_2+P}H + D_{\rm p}\nabla^2 P, \quad (1a)$$

$$\frac{\partial H}{\partial t} = \frac{C_1 P}{C_2+P}H - MH - F\frac{H^2}{C_3^2+H^2} + D_{\rm h}\nabla^2 H, \quad (1b)$$

where P is phytoplankton biomass, H is zooplankton biomass, $D_{\rm p}$ and $D_{\rm h}$ are the diffusion coefficients of phytoplankton and zooplankton, respectively. The parameters R, K, M, and $1/A_1$ denote respectively the intrinsic growth rate, carrying capacity of phytoplankton, the death rate, and yield coefficient of phytoplankton to zooplankton. F is the rate of zooplankton biomass consumed by fish per unit volume of water per day (average predation rate times the density of fish). The constants C_1, C_2, and C_3 parametrize the saturating functional response. It is simpler to work with Eq.(1) in rescaled dimensionless form via

$$t' = R_0 t, \quad r = \frac{R}{R_0}, \quad a = \frac{C_1 K}{C_2 R_0},$$
$$b = \frac{K}{C_2}, \quad m = \frac{M}{R_0},$$
$$n = \frac{C_3 A_1}{K}, \quad d_{\rm p} = \frac{k^2 D_{\rm p}}{L R_0},$$
$$d_{\rm h} = \frac{k^2 D_{\rm h}}{L R_0}, \quad f = \frac{F A_1}{C_3 R_0},$$

and t is used to represent t'. Here L and k denote respectively the total length of the area considered and the number of the nodes of the mesh for discretized space. The parameters r, a, b, m, n, $d_{\rm p}$, $d_{\rm h}$, and f have been defined in the previous works (see Refs.[10,11] for details). The dimensionless form of the system (1) is given by

$$\frac{\partial p}{\partial t} = rp(1-p) - \frac{ap}{1+bp}h + d_{\rm p}\nabla^2 p, \quad (2a)$$

$$\frac{\partial h}{\partial t} = \frac{ap}{1+bp}h - mh - f\frac{nh^2}{n^2+h^2} + d_{\rm h}\nabla^2 h. \quad (2b)$$

Here $p(x,y,t)$ and $h(x,y,t)$ are scalar fields representing the concentrations of phytoplankton species and zooplankton species respectively in the two-dimensional space. The local dynamics is given by

$$g_1(p,h) = rp(1-p) - \frac{ap}{1+bp}h, \quad (3a)$$

$$g_2(p,h) = \frac{ap}{1+bp}h - mh - f\frac{nh^2}{n^2+h^2}. \quad (3b)$$

The earlier results[46] about non-spatial system of model (2) by means of numerical bifurcation analysis showed that the bifurcation and bistability can

be found in system (2) when the parameters are varied within a realistic range. At the fixed parameters (see the caption of Figs.1 and 2), we can see that f controls the distance from Hopf bifurcation. For a larger f, there exists only one stable steady state. As f is decreased, the homogeneous steady state undergoes a saddle node (SN) bifurcation, that is $f_{\rm SN} = 0.658$. In this case, there exist a stable and an unstable steady states. Moreover, the bistability will emerge when the parameter f lies in the interval $f_{\rm SN} > f > f_{\rm c} = 0.445$ (this value is bigger than the Hopf onset, $f_{\rm H} = 0.3397$). There are three fixed points: the kinetic points A and C are linearly stable while point B is unstable (see Fig.1). Outside this interval, system (2) has a unique nontrivial equilibrium. Recent studies[11,29] showed that in system (2) the spiral waves can be well-developed in the oscillation regime, but the authors only considered the special case, i.e. $d_{\rm p} = d_{\rm h}$. To our knowledge, a few important issues have not yet been properly addressed such as the spatial pattern for $d_{\rm p} \neq d_{\rm h}$.

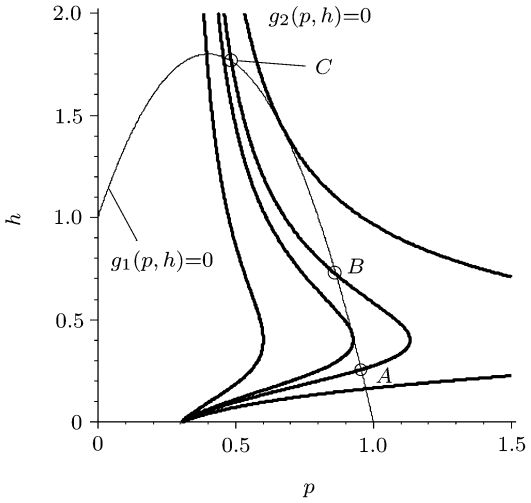


Fig.1. The diagram for the bistability and the Hopf bifurcation in system (3) with $r = 5.0$, $a = 5.0$, $b = 5.0$, $m = 0.6$, and $n = 0.4$. The thin curve is the $g_1(p,h)$. The thick curves are $g_2(p,h)$ with different values of f, corresponding to $f = 0.3$, $f = 0.445$, $f = 0.5$ and $f = 0.658$ from left to right.

Here we report the result of emergence of spatiotemporal chaos due to breakup in the system for the $d_{\rm h} \neq d_{\rm p}$ case. We may now use f and diffusion ratio, $\nu = d_{\rm h}/d_{\rm p}$, as control parameters to evaluate the region for the spiral wave. Turing instability in reaction–diffusion can be recast in terms of matrix stability.[48,49] With the help of Maple software assisted algebra computing, we obtain the parameters space (f,ν) bifurcation diagrams of the spiral waves as shown in Fig.2 in which three lines are plotted, one Hopf line (solid) and two Turing lines (dotted). In domain I, located above all the three bifurcation lines, the homogeneous steady states are the only stable solutions of the system. Domain II is the region of homogeneous oscillation in two-dimensional space.[47] In domain III, both Hopf and Turing instabilities occur, (i.e., mixed Turing–Hopf modes arise), in which the system generally produces the phase waves. Our results show that the system has spiral waves in this region. One can see that a Hopf bifurcation can occur in the steady state when the parameter f passes through its critical value $f_{\rm H}$ while the diffusion coefficients $d_{\rm p} = d_{\rm h} = 0$ and the bifurcation periodic solutions are stable. From our analysis (see Fig.2), one can also see that diffusion can induce Turing-type instability for the spatial homogeneous stable periodic solutions and the spatially extended model (2) exhibits spatiotemporal chaos patterns. The spatial pattern formation arises from the interaction between Hopf and Turing modes. It is interesting that the spiral wave and travelling wave will appear when the parameters, corresponding to the Turing–Hopf bifurcation region III in the spatially extended model (2), i.e., the Turing instability and Hopf bifurcation occur simultaneously.

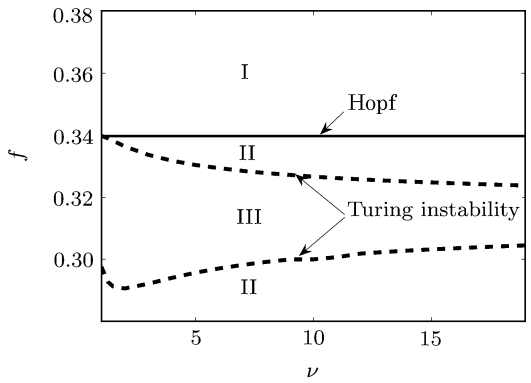


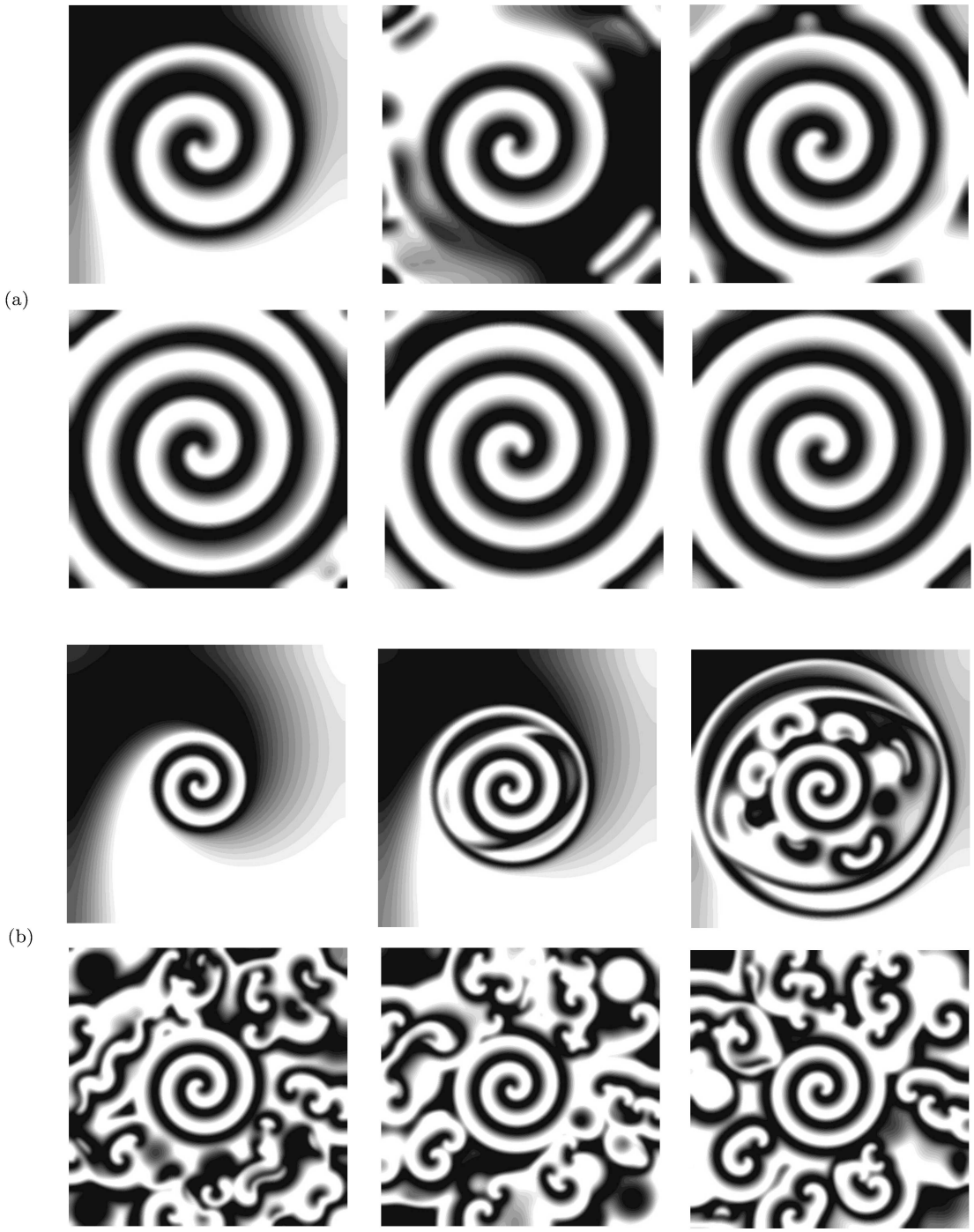
Fig.2. The sketch map of parameter space (f,ν) bifurcation diagrams for the spatially extended system (2) with $r = 5.0$, $a = 5.0$, $b = 5.0$, $m = 0.6$, $d_{\rm p} = 0.05$, and $n = 0.4$.

3. Numerical results

The simulation was done in a two-dimensional (2D) Cartesian coordinate system with a grid size of 600×600. We used the fourth order Runge–Kutta integrating method with a time step $\Delta t = 0.005$ time unit and a space step $\Delta x = \Delta y = 0.20$ length unit. Results remained the same when the reaction–diffusion equations were solved numerically in one and two spatial dimensions using a finite-difference approximation for the spatial derivatives and an explicit Euler method for the time integration. Neumann (zero-flux) boundary conditions were employed in our simulation. The diffusion terms in Eqs.(2a) and (2b) often describe the spatial mixing of species due to self-motion of the organism. The typical diffusion coefficient of plankton patterns d_{p} is about 0.05, which is based on the parameters estimated by Jørgensen and Bendoricchio[50] and Okubo,[51] using the relationship between turbulent diffusion and the scale of the space in the sea. In the previous studies,[10,11,29,33,46] a valuable insight into the role of spatial pattern for system (2) was provided if $d_{\mathrm{p}} = d_{\mathrm{h}}$. From an ecological viewpoint, it may be more practical when the diffusion coefficients satisfy $d_{\mathrm{h}} \geq d_{\mathrm{p}}$. However, here $d_{\mathrm{h}} < d_{\mathrm{p}}$ is also allowed since the natural waters turbulent diffusion dominates plankton mixing.[52] The other reasons for choosing such parameters (d_{h} and d_{p}) are that it is well-known new patterns, such as Turing patterns, can emerge in reaction–diffusion systems in which there is an imbalance between the diffusion coefficients d_{p} and d_{h}.[23,53] Therefore, we set $\nu = d_{\mathrm{h}}/d_{\mathrm{p}}$, and investigate whether a spiral wave would break up into complex spatiotemporal chaos when the diffusion ratio was varied. Throughout this paper, we fix $d_{\mathrm{p}} = 0.05$ and let d_{h} be a control parameter.

In the following, we will show that the dynamic behaviour of the spiral wave qualitatively changes as the control parameter d_{h} increases from zero, i.e., the diffusion ratio ν increases from zero to larger than one. For a large ν ($\nu > 1$), the outwardly rotating spiral wave is completely stable everywhere, and fills in the space when proper parameters are chosen, as shown in Fig.3(a). Figure 3(a) shows a series of snapshots of a well-developed single spiral wave formed spontaneously for the variable p in system (2). The spiral is initiated on a 600×600 grid by the cross-field protocol (the initial distribution is chosen in the form of allocated "constant-gradient" perturbation of the co-existent steady states), and zero boundary conditions are employed for simulations in two dimensions. From Fig.3(a) we can see that the well-developed spiral waves are formed first by the evolution. Inside the domain, new waves emerge, but are evolved by the spiral wave growing from the centre. The spiral wave can steadily grow and finally prevail over the whole domain (a movie illustrating the dynamical evolution for this case[54] [partly movie_1, movie_2, and movie_3 for $d_{\mathrm{h}} = 0.2$]). Figure 3(b) shows that the spiral wave first break up at a distance far away from the core centre, and eventually relatively large spiral fragments are surrounded by a 'turbulent' bath remain. The size of the surviving part of the spiral does not shrink when d_{h} further decreases until finally d_{h} equals 0, which is different from the phenomenon observed previously in the two-dimensional space Belousov–Zhabotinsky (BZ) and FitzHugh–Nagumo oscillatory system,[30,31,55–57] in which the breakup gradually invades the stable region near the core centre, and finally the spiral wave breaks up throughout the whole medium. Figure 3(c) is the time sequences (arbitrary units) of the variables p and h at an arbitrary spatial point within the spiral wave region, from which we can see that the spiral waves are caused by the accepted as "phase waves" with substantial group velocity, phase velocity and sinusoidal oscillation rather than the relaxational oscillation with large amplitude. This breakup scenario is similar to the breakup of rotating spiral waves observed in numerical simulations in chemical systems,[30,31,55–57] and experiments in BZ systems,[58,59] showing that spiral wave breakup in these systems is related to the Eckhaus instability and, more importantly, the absolute instability. The corresponding trajectories of the spiral core and the spiral arm (far away from the core centre) at $y = 300$ are shown in Fig.4. From Fig.4, we can see that the spiral core is not completely fixed, but oscillates with a large amplitude. However, as d_{h} decreases to a critical value, an unstable modulation develops in regions which are far away from the spiral core (see the middle panel of Fig.4(b)). These oscillations eventually grow large enough to cause the spiral arm far away from the core to breakup into complex multiple spiral waves, while the core region remains stable (the corresponding movie can be viewed in the online supplemental movies[54] [partly movie_1 and movie_2, and for $d_{\mathrm{h}} = 0.02$]). Figures 3(b) and 4(b) show the dynamic behaviour for $d_{\mathrm{h}} = 0.02$, i.e., $\nu = 0.4$. The regular trajectories far away from the core are now the same as the region of the spatial chaos (see the

middle panels of Figs.4(a) and 4(b)). It is shown that a decreased diffusion ratio ν leads to the increment of amplitude (see the left panels of Figs.4(a) and 4(b)). As is well known, the minimum value of the population density decreases, and species extinction is expected to be more probable due to stochastic environmental perturbations. Thus, the amplification of amplitude indicates a large extinctive risk for species. However, from the spatial evolution of system (2) (see Fig.3), the temporal variations of the density in different areas can become asynchronous and the local extinction can be compensated due to re-colonization (or diffusion) from neighbouring areas.



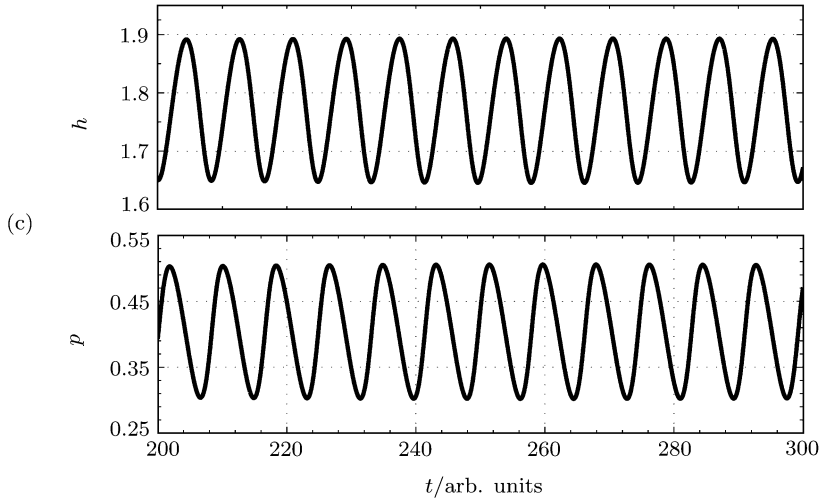


Fig.3. Well-developed spiral waves and some properties of them. The figures show results of simulations for system (2) with $r = 5$, $a = 5$, $b = 5$, $m = 0.6$, $n = 0.4$, $d_{\rm p} = 0.05$, and $f = 0.3$. (a) Well developed spiral waves shown at subsequent snapshot in time, $d_{\rm h} = 0.2$. (b) Far-field breakup of the spiral waves shown at subsequent snapshot in time, $d_{\rm h} = 0.002$. The white (black) areas correspond to maximum (minimum) values of p (additional movie format available in Ref.[54]). (c) Oscillations of the variables p and h at an arbitrary spatial point within the regular spiral wave region for both scenarios. Each figure is taken at a long time until spatial patterns are unchanged.

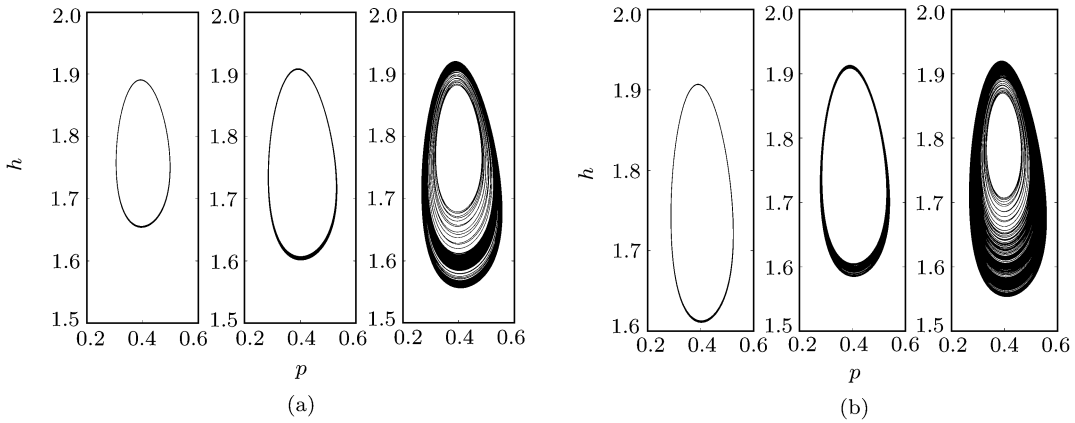


Fig.4. The corresponding trajectories (from left to right) for locations $(300, 300)$, $(250, 300)$, and $(50, 300)$. The parameters in (a) and (b) are the same as those in Figs.3(a) and 3(b), respectively.

Furthermore, it is well known that a basic argument in spiral stability analysis can be carried out by reducing the system to one-dimensional space.[30,31,57−57] Here we show some essential properties of the spiral breakup from the results of numerical simulation. In this model, it is worth noticing that the oscillation of the dynamics in the core cannot be neglected due to the system exhibiting spatial periodic wave trains solutions in one-dimensional space, as shown in Fig.5. Breakup occurs first far away from the core (the source of waves). The spiral wave breaks towards the core until it approaches a constant distance and then the surviving part of the spiral wave becomes stable. The minimal stable wavelength is called $\lambda_{\rm min}$. So the one-parameter family may be described by a dispersion curve $\lambda(d_{\rm h})$ (see Fig.6). The minimal stable wavelength $\lambda_{\rm min}$ of the spiral waves is shown in Fig.6 obtained from simulation in two-dimensional space. The results of Fig.6 can be interpreted as follows: the minimal stable wavelength decreases with the decrease of $d_{\rm h}$ and eventually levels out at a relative constant value, at which a stable spiral wave can exist for a larger region of $d_{\rm h}$. Space-time plots at different times are shown in Fig.5 for two different $d_{\rm h}$ values (i.e., different ν), which display the time evolution of the spiral waves along the cross section in

the two-dimensional images of Figs.3(a) and 3(b). As shown in Figs.5(a) and 5(b) for $d_{\rm h} = 0.2$ and 0.02 respectively, the waves display unstable modulated perturbation far away from the core due to convective instability,[30,31,55−57] but this perturbation is gradually advected to the left and right sides, and finally disappears. The instability manifests the production of the wave train breakup into several waves from far-field, as shown in Fig.5(b).

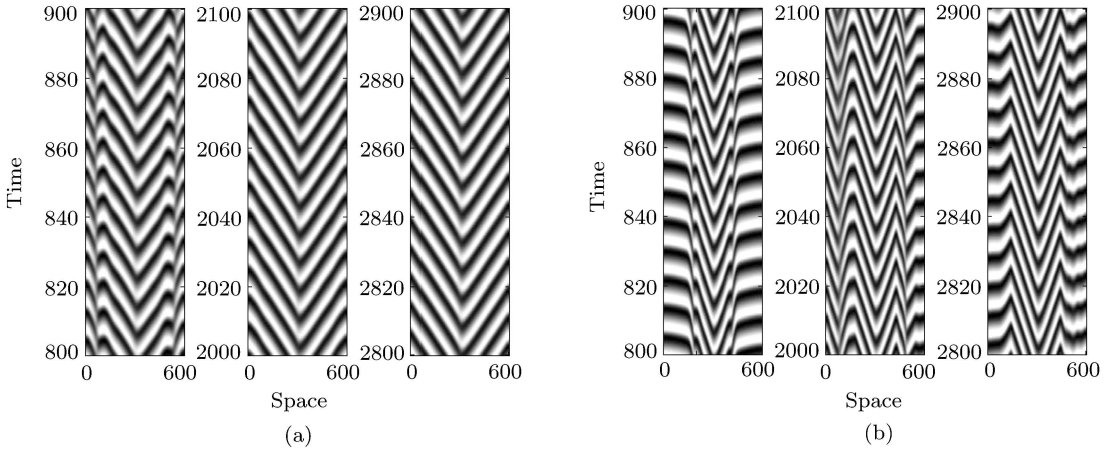


Fig.5. Space-time plots of variable p for different time and $d_{\rm h}$. The parameters in (a) and (b) are the same as those in Figs.3(a) and 3(b), respectively.

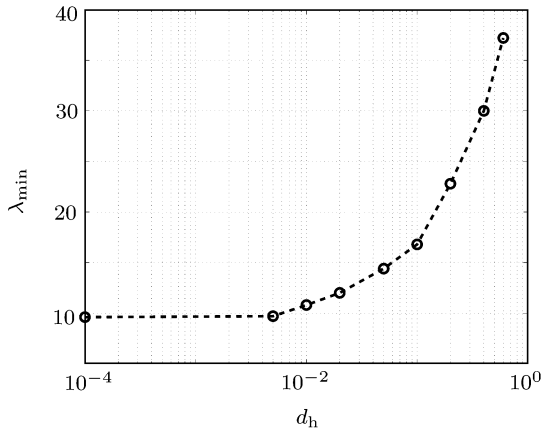


Fig.6. Dependence of the wavelength $\lambda_{\rm min}$ on the parameter $d_{\rm h}$ for system (2) with $r = 5.0$, $a = 5.0$, $b = 5.0$, $m = 0.6$, $d_{\rm p} = 0.05$, and $n = 0.4$. Note the log scale for $d_{\rm h}$.

4. Nonlinear bifurcation of the spiral waves

In practice, such computations as above only require discretization in one-dimensional space and comparison with computing eigenvalues of the full stability problem on a large domain due to the spiral waves exhibiting travelling waves in the plane (see Fig.5 about the space-time graphs). For the sake of simplicity, Eqs.(2a) and (2b) can be written as follows:

$$\frac{\partial p}{\partial t} = d_{\rm p}\nabla^2 p + g_1(p,h), \tag{4a}$$

$$\frac{\partial h}{\partial t} = d_{\rm h}\nabla^2 h + g_2(p,h). \tag{4b}$$

The homogeneous stationary solutions of system (4) can be obtained by setting Laplacian operators to 0. If the homogeneous steady-state is destabilized, then its linearization will accommodate waves in the form $\mathrm{e}^{\mathrm{i}(kx-\omega t)}$ for certain values of k and ω. Typically, near the transition to instability, small spatially periodic travelling waves arise for any wave number close to $k_{\rm c}$, which is the critical wave number. Their wave speed is approximately equal to $\dfrac{\omega_{\rm c}}{k_{\rm c}}$. In this paper, we focus exclusively on the situation where $\omega_{\rm c} = 0$ and $k_{\rm c} \neq 0$. The bifurcation with $\omega_{\rm c} = 0$ and $k_{\rm c} \neq 0$ is known as the Turing bifurcation, and the bifurcating spatially periodic steady patterns are often referred to as Turing patterns. Another class of moving patterns will appear when the instabilities are modulated by Hopf-Turing bifurcation, which resembles travelling waves. Moreover, the common feature of spiral waves in one-dimensional space mentioned above is the presence of wave trains which are spatially periodic travelling waves in the form $p_{wt}(kx - \omega t; k)$ and $h_{wt}(kx - \omega t; k)$, where $p_{wt}(\phi; k)$ and $h_{wt}(\phi; k)$ are 2π-periodic about ϕ. Typically, the spatial wave number

k and the temporal frequency ω are related via the nonlinear dispersion relation $\omega = \omega(k)$ so that the phase velocity is given by

$$c_{\mathrm{p}} = \frac{\omega}{k}. \tag{5}$$

A second quantity related to the nonlinear dispersion relation is the group velocity of the wave train, $c_{\mathrm{g}} = \dfrac{\mathrm{d}\omega}{\mathrm{d}k}$, which also plays a central role in the spiral waves. The group velocity c_{g} gives the speed of propagation of small localized wave-package perturbations of wave train.[60] Here, we only focus on the existence of the travelling wave solution. In fact, the spiral waves move at a constant speed outward from the core (see Fig.5), so that they have the mathematical form $p(x,t) = P(z)$, and $h(x,t) = H(z)$ where $z = x - c_{\mathrm{p}}t$. Substituting these solution forms into Eq.(4), we obtain the following ODEs

$$d_{\mathrm{p}}\frac{\mathrm{d}^2P}{\mathrm{d}z^2} + c_{\mathrm{p}}\frac{\mathrm{d}P}{\mathrm{d}z} + g_1(P,H) = 0, \tag{6a}$$

$$h_{\mathrm{p}}\frac{\mathrm{d}^2H}{\mathrm{d}z^2} + c_{\mathrm{p}}\frac{\mathrm{d}H}{\mathrm{d}z} + g_2(P,H) = 0. \tag{6b}$$

We will investigate numerically the existence, speed and wavelength of travelling wave patterns. Our approach is to use the bifurcation package Matcont2.4[61] to study system (6). To do this, the most natural bifurcation parameters are the wave speed c_{p} and f, but they give no information about the stability of travelling waves as solutions of PDEs model (4).

Our starting point is the homogeneous steady state of Eq.(6) within domain III in Fig.2. The typical bifurcation diagrams are illustrated in Fig.7, which shows that a steady spatially periodic travelling wave can exist for a larger value of the speed c_{p}, but it is unstable for a small value of c_{p}. The changes of stability occur via Hopf bifurcation, from which a branch of periodic orbits emanates. Note that here we use the terms 'stable' and 'unstable' to refer to the ODEs system (6) rather than the PDEs model (2). Figure 7(b) illustrates the maximum stable wavelength against the bifurcation parameter (speed c_{p}),

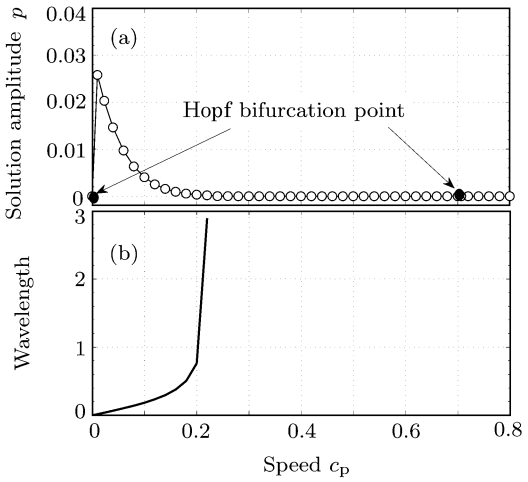


Fig.7. Typical bifurcation diagrams for the pattern ODEs (6). (a) The spatial periodic travelling waves of system (4). The changes of stability occur via Hopf bifurcation, from which a branch of periodic orbits emanates. Thus unstable travelling waves appear. (b) Maximum stable wavelength along the bifurcation parameter c_{p}, i.e., $k \neq 0, \omega \neq 0$. The parameter values in (a) and (b) are the same as in Fig.3(a).

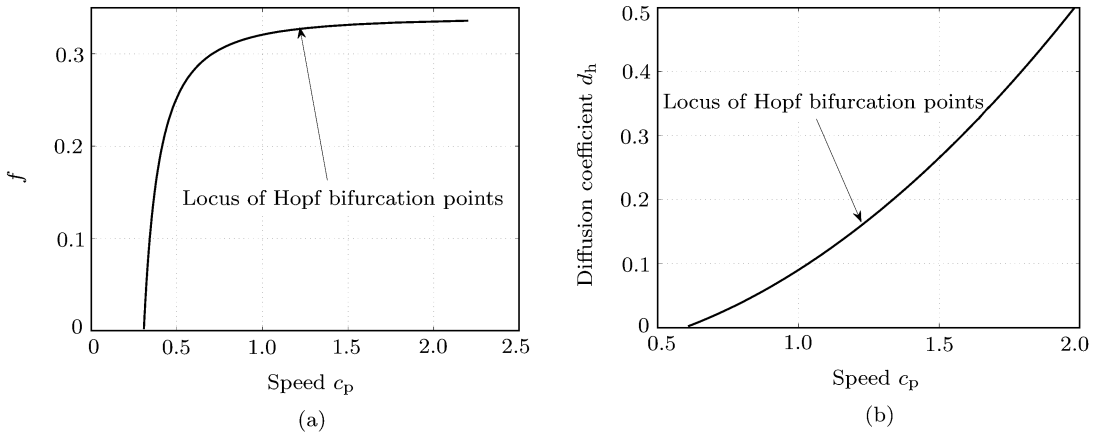


Fig.8. An illustration of the variation in parameters space of the ODEs (6). We plot the loci of Hopf bifurcation points. (a) $f - c_{\mathrm{p}}$ plane; (b) $d_{\mathrm{h}} - c_{\mathrm{p}}$ plane. The parameter values in (a) and (b) are the same as in Fig.3(a).

and these amplitudes have a very long wavelength. It is known that $c_{\rm p} = \dfrac{\omega}{k}$, hence the travelling wave solution exists when $c_{\rm p} \neq 0$ (i.e. $k \neq 0, \omega \neq 0$). Using Matcont2.4 package, it is possible to track the locus of Hopf bifurcation points and the limit point (fold) bifurcation on two parameters plane. A typical examples of $c_{\rm p} - f$ and $c_{\rm p} - d_{\rm h}$ planes are illustrated in Fig.8. The travelling wave solutions exist when $c_{\rm p}$ and f lying in the left of Hopf bifurcation locus (see Fig.8(a)). The similar structure obtained about $c_{\rm p} - d_{\rm h}$ plane is shown in Fig.8(b). These results extend our previous analysis coming from the algebraic calculation (see Fig.2) and numerical results (see Fig.5).

5. Conclusions and discussion

We have investigated a spatially extended plankton ecosystem in two-dimensional space and found that its spatial patterns exhibit spiral waves dynamics and spatial chaotic structures. Specifically, the scenario of spatiotemporal chaotic patterns arising from the far-field breakup is revealed in the present paper. Our study is based on numerical analysis of a kinematic mimicking for marine organisms with diffusion, by coupling two-component plankton model on levels of ecological organization. By changing (increasing or decreasing) the diffusion ratio of two variables, we find that the spiral wave's arm first breaks up into a turbulence-like pattern at places far away from the core centre, but it does not invade the whole space. The far-field breakup may be verified in field observation and useful in understanding the population dynamics in oceanic ecosystems. For instance, it has been reported that the interplay between wake (or ocean) structures and biological growth leads to plankton blooms inside the mesoscale hydrodynamic vortices, which act as an incubator of primary production,[62,63] as well as the large-scale regular spatial patterns in young mussel beds.[64,65] We see that spatial periodic blooms appear in phytoplankton populations (see Fig.3). The spatial evolution of phytoplankton population during one bloom cycle can be seen from the corresponding movies.[54]

Garvie and Trenchea[29] have studied the optimal control problem of model (2) from spatiotemporal chaos to spiral waves, in which the fish predation is treated as a multiplicative control variable. It is well known that spatial order emerges in a range of spatial models for multi-species interactions. Spatial models of multi-species often manifest very different behaviours from their mean-field counterparts. They exhibit two important general features. One is that they allow the possibility of global persistence in spite of local extinctions and so the spatial models are usually more stable than their mean-field equivalents. The other is that they have a tendency to spatial self-organization or regular spatiotemporal patterns.[14,66] The spatial structure produces non-random spatial patterns such as spiral waves and spatiotemporal chaos at scales much larger than the scale of interaction among individuals level. These structures are not explicitly revealed but emerge from local interaction among individuals and local diffusion as well.

We have known that plankton plays an important role in marine ecosystem and climate, because of its participation in the global carbon and nitrogen cycle at the base of food chain.[67] Many recently-developed ecosystem models incorporate different phytoplankton functional groups and their competition for light and multiple nutrients.[68] Simulations of these models in specific areas suggest that changes of global environment, including global-warming-induced changes, will alter phytoplankton community structure and hence alter global biogeochemical cycles.[69] The coupling of spatial ecosystem model to global climate poses a series of open questions on the complexity of ecosystem and relevant spatial scales. So the study of spatial model in large-scale space is becoming more important in the ecology. Based on numerical simulation of the spatial model, we can conclude that the oceanic ecological systems show permanent spiral waves and spatiotemporal chaos in large-scale space over a range of parameter values $d_{\rm h}$, indicating that periodically sustained plankton blooms in the local area. To test our results, the most powerful empirical approach is to conduct experiments in which the spatial pattern can be measured directly, but it is difficult to design them. However, we can indirectly study these phenomena by simulation and comparison with the satellite pictures. For example, the spatiotemporal chaotic patterns agree with the perspective observed of Fig.3 in Ref.[68]. Also, some satellite imageries (http://oceancolor.gsfc.nasa.gov) have displayed spiral patterns that represent the phytoplankton (the chlorophyll) biomass, and thus demonstrated that plankton patterns in ocean occur on much broader scales, therefore such mechanisms as regarded as diffusion should be considered.

References

[1] Amritkar R E and Rangarajan G 2006 *Phys. Rev. Lett.* **96** 258102
[2] Pekalski A and Droz M 2006 *Phys. Rev.* E **73** 021913
[3] Sayama Y Y H, de Aguiar M A M and Baranger M 2003 *FORMA* **18** 19
[4] Gilad E, von Hardenberg J, Provenzale A, Shachak M and Meron E 2004 *Phys. Rev. Lett.* **93** 098105
[5] Washenberger M J, Mobilia M and Täuber U C 2007 *J. Phys.: Cond. Matt.* **19** 065139
[6] Mobilia M, Georgiev I and Täuber U 2007 *J. Stat. Phys.* **128** 447
[7] Blasius B, Huppert A and Stone L 1999 *Nature* **399** 354
[8] von Hardenberg J, Meron E, Shachak M and Zarmi Y 2001 *Phys. Rev. Lett.* **87** 198101
[9] Provata A and Tsekouras G A 2003 *Phys. Rev.* E **67** 056602
[10] Medvinsky A B, Tikhonova I A, Aliev R R, Li B L, Lin Z S and Malchow H 2001 *Phys. Rev.* E **64** 021915
[11] Medvinsky A B, Petrovskii S V, Tikhonova I A, Malchow H and Li B L 2002 *SIAM Review* **44** 311
[12] Gurney W S C, Veitch A R, Cruickshank I and McGeachin G 1998 *Ecology* **79** 2516
[13] Murray J D 2002 *Mathematical Biology* (New York: Springer, 3rd edn) p71
[14] Petrovskii S, Li B L and Malchow H 2004 *Ecological Complexity* **1** 37
[15] Armi L, Hebert D, Oakey N, Price J, Richardson P L, Rossby T and Ruddick B 1988 *Nature* **333** 649
[16] Ranta E, Kaitala V and Lundberg P 1997 *Science* **278** 1621
[17] Luckinbill L S 1974 *Ecology* **55** 1142
[18] Holyoak M 2000 *J Anim. Ecol.* **69** 985
[19] Jansen V A A 1995 *Oikos* **74** 384
[20] Jansen V A and Lloyd A L 2000 *J. Math. Biol.* **41** 232
[21] Jansen V A 2001 *Theor. Popul. Biol.* **59** 119
[22] Allen J C, Schaffer W M and Rosko D 1993 *Nature* **364** 229
[23] Cross M C and Hohenberg P C 1993 *Rev. Mod. Phys.* **65** 851
[24] Lee K J, Goldstein R E and Cox E C 2001 *Phys. Rev. Lett.* **87** 068101
[25] Sawai S, Thomason P A and Cox E C 2005 *Nature* **433** 323
[26] Winfree A T 1991 *Chaos* **1** 303
[27] Biktashev V N, Brindley J, Holden A V and Tsyganov M A 2004 *Chaos* **14** 988
[28] Garvie M R 2007 *Bull. Math. Biol.* **69** 931
[29] Garvie M R and Trenchea C 2007 *SIAM J. Contr. and Opti.* **46** 775
[30] Bär M and Brusch L 2004 *New J. Physics* **6** 5
[31] Bär M and Or-Guil M 1999 *Phys. Rev. Lett.* **82** 1160
[32] Johnson C R and Boerlijst M C 2002 *Trends Ecol. and Evol.* **17** 83
[33] Pascual M 1993 *Procc. R. Soc. Lond.* B **251** 1
[34] Sherratt J A, Eagan B T and Lewis M A 1997 *Phil. Trans. R. Soc. Lond. B* **352** 21
[35] Petrovskii S V and Malchow H 2001 *Theor. Popul. Biol.* **59** 157
[36] Sherratt J A 2001 *Ecol. Lett.* **4** 30
[37] Savill N J and Hogeweg P 1998 *Proc. R. Soc. Lond.* B **265** 25
[38] Abraham E R 1998 *Nature* **391** 577
[39] Folt C L and Burns C W 1999 *Nature* **14** 300
[40] Scheffer M 1991 *J. Plankton Res.* **13** 1291
[41] Hanski I, Turchin P, Korplmakl E and Henttonen H 1993 *Nature* **364** 232
[42] Ellner S and Turchin P 1995 *Am. Nat.* **145** 343
[43] Dennis B, Desharnais R A, Cushing J M, Henson S M and Costantino R F 2001 *Ecol. Monogr.* **71** 277
[44] Becks L, Hilker F M, Malchow H, Jorgens K and Arndt H 2005 *Nature* **435** 1226
[45] Scheffer M 1991 *Oikos* **62** 271
[46] Malchow H 1993 *Procc. R. Soc. Lond.* B **251** 103
[47] Liu Q X, Jin Z and Li B L 2008 *J Stat. Mech.* **2008** P05011
[48] Scheel A 2003 *Mem. Amer. Math. Soc.* **165** 86
[49] Satnoianu R A, Menzinger M and Maini P K 2000 *J. Math. Biol.* **41** 493
[50] Jørgensen S E and Bendoricchio G 2001 *Fundamentals of Ecological Modelling.*(Amsterdam: Elsevier, 3rd edn) p62
[51] Okubo A 1980 *Diffusion and Ecological Problems: Mathematical Models* (Berlin: Springer) p238
[52] Sugihara G and May R M 1990 *Nature* **344** 734
[53] Turing A M 1952 *Phil. Trans. R. Soc. Lond.* B **237** 37
[54] See the movie for the evolution online at http://7y.nuc.edu.cn/jinzhen/English1.aspx
[55] Xie F, Xie D and Weiss J N 2006 *Phys. Rev.* E **74** 026107
[56] Sandstede B and Scheel A 2000 *Phys. Rev.* E **62** 7708
[57] Tobias S M and Knobloch E 1998 *Phys. Rev. Lett.* **80** 4811
[58] Ouyang Q and Flesselles J M 1996 *Nature* **379** 143
[59] Ouyang Q, Swinney H L and Li G 2000 *Phys. Rev. Lett.* **84** 1047
[60] Sandstede B and Scheel A 2004 *SIAM J. Appl. Dynam. Syst.* **3** 1
[61] Dhooge A, Govaerts W, Kuznetsov Y A, Mestrom W, Riet A M and Sautois B 2006 *Matcont and Cl-Matcont: Continuation Toolboxes in Matlab* (Utrecht University, The Netherlands) p48
[62] Sandulescu M, Lópes C, Hernández-Garc´ia E and Feudel U 2007 *Nolin. Proc. Geophys.* **14** 443
[63] Sandulescu M, Lópes C, Hernández-Garc´ia E and Feudel U 2007 *Geophys. Research Abstracts* **9** 09533
[64] van de Koppel J, Rietkerk M, Dankers N and Herman P M J 2005 *Am. Nat.* **165** e66
[65] Wang R H, Liu Q X, Sun G Q, Jin Z and van de Koppel J 2008 *Journal of the Royal Society Interface* 0349
[66] Dieckmann U, Law R and Metz J A J 2000 *The Geometry of Ecological Interactions: Simplifying Spatial Complexity* (Cambridge: Cambridge University Press) p171–182
[67] Duinker J and Wefer G 1994 *Naturwissenschaften* **81** 237
[68] Pascual M 2005 *Plos. Comput. Biol.* **1** 101
[69] Litchman E, Klausmeier C A, Miller J R, Schofield O M and Falkowski P G 2006 *Biogeosciences* **3** 585